Asia-Pac. J. Atmos. Sci., 54(1), 33-41, 2018
DOI:10.1007/s13143-017-0057-9

pISSN 1976-7633 / eISSN 1976-7951

Investigation of Primary Factors Affecting the Variation of Modeled Oak Pollen Concentrations: A Case Study for Southeast Texas in 2010

Wonbae Jeon[1], Yunsoo Choi[1], Anirban Roy[1], Shuai Pan[1], Daniel Price[2], Mi-Kyoung Hwang[3], Kyu Rang Kim[4], and Inbo Oh[5]

[1]*Department of Earth and Atmospheric Sciences, University of Houston, Houston, TX, USA*
[2]*Honors College, University of Houston, Houston, TX, USA*
[3]*Division of Earth Environmental System, Pusan National University, Busan, Korea*
[4]*Applied Meteorology Research Division, National Institute of Meteorological Sciences, Jeju, Korea*
[5]*Environmental Health Center, University of Ulsan College of Medicine, Ulsan, Korea*

(Manuscript received 9 October 2016; accepted 5 May 2017)

Abstract: Oak pollen concentrations over the Houston-Galveston-Brazoria (HGB) area in southeastern Texas were modeled and evaluated against in-situ data. We modified the Community Multi-scale Air Quality (CMAQ) model to include oak pollen emission, dispersion, and deposition. The Oak Pollen Emission Model (OPEM) calculated gridded oak pollen emissions, which are based on a parameterized equation considering a plant-specific factor (C_e), surface characteristics, and meteorology. The simulation period was chosen to be February 21 to April 30 in the spring of 2010, when the observed monthly mean oak pollen concentrations were the highest in six years (2009-2014). The results indicated C_e and meteorology played an important role in the calculation of oak pollen emissions. While C_e was critical in determining the magnitude of oak pollen emissions, meteorology determined their variability. In particular, the contribution of the meteorology to the variation in oak pollen emissions increased with the oak pollen emission rate. The evaluation results using in-situ surface data revealed that the model underestimated pollen concentrations and was unable to accurately reproduce the peak pollen episodes. The model error was likely due to uncertainty in climatology-based C_e used for the estimation of oak pollen emissions and inaccuracy in the wind fields from the Weather Research and Forecast (WRF) model.

Key words: Oak pollen, Southeast Texas, pollen model, CMAQ, pollen dispersion

1. Introduction

Several studies have illustrated the deleterious health effects of pollen, which include allergic airway diseases such as rhinoconjunctivitis and asthma, with the most prevalent impacts among children and adolescents (Nathan et al., 1997; Taylor et al., 2007). These diseases cause significant productivity loss and increased stress on health care resources (Schoenwetter et al., 2004; Lamb et al., 2006). Therefore, it is imperative to understand the processes influencing pollen concentrations in the atmosphere.

Previous studies have performed pollen forecasting using Gaussian (Pfender et al., 2007), Lagrangian (Jarosz et al., 2004; Pasken and Pietrowicz, 2005) and Eulerian models (Dupont et al., 2006). A couple of studies have focused on the dispersion of pollen emissions from specific tree types such as birch and oak (Schuler and Schlünzen, 2006; Vogel et al., 2008; Verinakaite et al., 2010). In this space, it is preferable to use a chemical transport model, since it can simultaneously calculate the concentrations of co-stressors such as gaseous and particle-phase of air pollutants. These include nitrogen dioxide, ozone, and diesel exhaust particles which have been known to enhance the deleterious health effects of pollen (e.g., Knox et al., 1997; Motta et al., 2006; Després et al., 2012).

There have been a couple of chemical transport model evaluations of pollen in different regions. For example, Helbig et al. (2004) developed parameterizations for the estimation of vertical pollen emission flux which take into account plant-specific factors, friction velocity, and meteorology. They implemented these parameterizations in the KAMM/DRAIS model (Vogel et al., 1995) and simulated pollen counts in Germany. Efstathiou et al. (2011) implemented the parameterizations described by Helbig et al. (2004) in the Community Multiscale Air Quality model (CMAQ) and conducted pollen modeling over the northeastern United States (US). Zink et al. (2013) introduced a new pollen emission parameterization which takes into account plant-specific variables, meteorology, and turbulent kinetic energy. They implemented it into the Consortium for Small-scale Modeling - Aerosols and Reactive Trace Gases (COSMO-ART) modeling system (Vogel et al., 2009) and simulated birch pollen concentrations in central Europe. Although these studies have indicated reliable modeling performance, most of them focused on European regions, and only a few studies considered modeling pollen concentrations in the US, where the tree species distribution is significantly different from Europe and highly variable across the country. Especially, to the best of our knowledge, no literature on the pollen prediction over the southern US, Texas from a 3-dimensional chemical transport model have been reported so far. The model predictions and performance over this region could potentially be different from the previous studies, due to

Corresponding Author: Inbo Oh, Environmental Health Center, University of Ulsan College of Medicine, Ulsan 44033, Korea.
E-mail: oinbo@ulsan.ac.kr

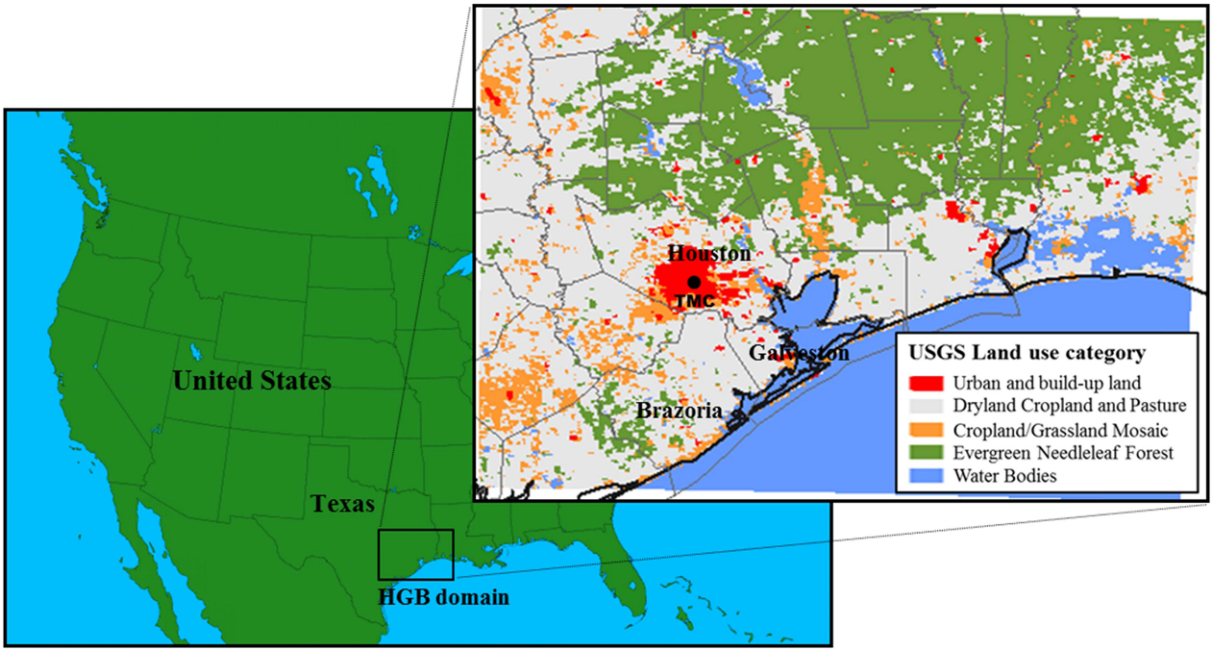

Fig. 1. Location of modeling domain (HGB) in this study. The right panel shows the distribution of land-use types inside the HGB domain. The symbol (●) represents the location of Texas Medical Center (TMC) pollen measurement site.

the complexity in the dependence of pollen flux on specific tree types and locations.

This study proposes to model springtime oak pollen concentrations over southeastern Texas using a chemical transport model. We chose Oak since it is the predominant species over a given urban site in Houston, as explained in the Methodology. Here, we simulate oak pollen emissions and concentrations and investigate the primary causes behind their variability and model measurement error. In this space, an emission model based on the parameterizations described by Efstathiou et al. (2011) is employed to simulate oak pollen emissions, and the estimated emissions are used as input for CMAQ. This study focuses on evaluating the modeling performance for oak pollen simulation in the southeastern Texas region and investigating the primary factors affecting the model-measurement error. Thus, we ultimately improve the pollen modeling system for more accurate modeling purposes.

2. Model description

a. Oak pollen emission model

We chose oak pollen as the study species based on the measured pollen counts at the Texas Medical Center (TMC) site in Houston (Fig. 1) over a six year (2009-2014) period. The measurements indicated that oak pollen was the predominant contributor by pollen count (52.57%), followed by pine (15.85%), ashe juniper/bald cypress (11.90%) and elm (7.13%). Hence, an emission model for oak pollen (Oak Pollen Emission Model, OPEM, hereafter) was developed to estimate its emission flux over Southeast Texas. The model generates gridded hourly oak pollen emissions for a specific modeling domain. The OPEM utilizes a parameterized equation for the estimation of emission flux of oak pollen particles, which is based on the findings by Helbig et al. (2004) and Efstathiou et al. (2011). The comparison of the other recent parameterizations with Efstathiou et al. (2011) was reported by Zink et al. (2013), but their reliable performance for the US domain has not been clearly demonstrated. Thus, the parameterization described by Efstathiou et al. (2011), which already showed reasonable pollen modeling results in the US domain was employed in this study. The hourly averaged vertical emission flux of pollen particles (F_p) at the top of the vegetation canopy was parameterized as shown below,

$$F_p = C_e \cdot c^* \cdot K_e \cdot u_* \cdot w_f \quad (1)$$

It is assumed the pollen flux F_p ($m^{-2}\ s^{-1}$) is proportional to the dimensionless plant-specific factor (C_e), characteristic concentration (c^*), dimensionless meteorological adjustment factor (K_e), grid cell averaged frictional velocity (u_*) and a cell averaged weighting factor (w_f).

The factor C_e describes the flowering stage of oak pollen. It represents the amount of pollen produced with time during the flowering period and is dependent on the type of pollen species and geographical features of target area (Rojo and Perez-Badia, 2015). We used a climatologic approach based on the parameterization described by Helbig et el. (2004) and Oh et al. (2012) to determine C_e for this study. Defining and using a specific C_e for each year would produce accurate simulation

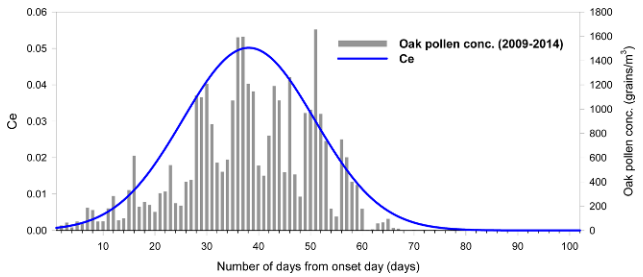

Fig. 2. Variation of observed oak pollen concentrations after the onset day. The concentrations are averages for six years (2009-2014), and the curve represents normal distribution.

results, but they would not be able to be used for forecasting purpose. For this study, the characteristics of observed oak pollen concentrations post-blooming (onset day) in Houston during the recent six years (2009-2014) were analyzed to define a representative C_e factor. The data roughly approximated a normal distribution curve:

$$C_e = 1.6\frac{1}{\sigma\sqrt{2\pi}}e^{-\frac{(d-\mu)^2}{2\sigma^2}} \quad (2)$$

Where d is the number of days after onset, σ is 12.72 (days^2) and μ is 38.1 days. Figure 2 plots the variation in oak pollen concentration post-onset day and its fitted distribution curve.

The factor c^* is calculated as:

$$c^* = \frac{p^q}{LAI \cdot h^c} \quad (3)$$

where p^q is the total amount of oak pollen produced per square meter in one season, LAI and h^c are leaf area index and canopy height respectively. The value of p^q considered in this study is 8.814×10^9, calculated by multiplying the average number of pollen grains per tree (2.6×10^{10} grains tree^{-1} yr^{-1}) (Jato et al., 2007) by the number of standing oak trees per hectare (3,390 trees ha^{-1}) (Saito et al., 2006). The gridded LAI values were calculated by the Weather Research and Forecasting (WRF, Version 3.6.1) model and the h^c value was set to 6.38 m. This is the mean canopy height in Houston area reported by Burian et al. (2004). The value of u_* was calculated by the WRF model.

The factor K_e represents resistance against the pollen release due to meteorological conditions, given by:

$$K_e = 1 - \frac{3}{c_1\frac{T}{T_{te}} + c_2\frac{WS}{WS_{te}} + c_3\frac{RH_{te}}{RH}} \quad (4)$$

where, T, WS, and RH are air temperature, wind speed, and relative humidity respectively. We assigned the first-layer gridded outputs from the WRF simulation to each meteorological parameter. T_{te}, WS_{te} and RH_{te} are threshold values for air temperature, wind speed, and relative humidity; while c_1, c_2 and c_3 are weighting factors for their corresponding meteorological resistances (Helbig et al., 2004; Oh et al., 2012). The

Table 1. Configuration and detailed physical options for WRF simulation.

Number of grids	95 × 77
Horizontal resolution	4 km
Vertical layers	33 layers
Initial data	The North American Regional Reanalysis (NARR)
Microphysics option	WSM 3-class simple ice scheme
Radiation option	RRTM (long wave) / Dudhia (short wave) scheme
Surface layer option	Monin-Obukhov (Janic Eta) scheme
Land-surface option	Unified Noah land-surface model
PBL option	YSU scheme
Cumulus option	Kain-Fritsch (new Eta) scheme

Table 2. Same as Table 1, but for CMAQ.

Meteorology	WRF
Number of grids	84 × 66
Horizontal resolution	4 km
Vertical layers	27 layers
Chemical mechanism	CB05 (gas-phase) / AERO6 (aerosol)
Chemical solver	SMVGEAR
Horizontal advection	Yamo
Horizontal diffusion	Multiscale
Vertical advection	WRF
Vertical diffusion	ACM2
Deposition	M3dry
Emissions inventory	NEI 2011

threshold values for K_e were taken to be: $T_{te} = 8.0$°C, $WS_{te} = 2.5$ m s^{-1}, and $RH_{te} = 90\%$. The weighting factors were determined as $c_1 = 0.5$, $c_2 = 2.0$, and $c_3 = 1.0$ to consider the relative importance of each meteorological parameter on the variation of oak pollen concentration. The factor w_f assumes annual variation in pollen production due to climate of the preceding year and biological rhythms (Stanley and Linkens, 2012). This factor was not taken into account in this study (i.e., $w_f = 1$) because of lack of measurement data, which are needed to determine the specific weighting factor for the Houston-Galveston-Brazoria (HGB) area.

b. Oak pollen simulation model

The United States Environmental Protection Agency (USEPA)'s Community Multiscale Air Quality (CMAQ) model (Byun and Schere, 2006) version 5.0.1 was modified to include oak pollen as a model species. This framework was called the CMAQ-Pollen Modeling System (CPM, hereafter) and is based on the original version of CMAQ utilized by the authors in previous studies (e.g., Diao et al., 2016; Pan et al.,

2015; Pan et al., 2017). We introduced pollen into the model as a coarse-particle species (PM_{10}). It was assumed to be non-reactive since the reactions of pollen with other pollutants have not been well documented. The OPEM- emissions were added into the CMAQ-ready emissions inventory modeled using the Sparse Matrix Operator Kernel Emissions (SMOKE, Ver. 3.6) model (Houyoux et al., 2000).

The WRF simulations provided the gridded meteorological fields needed as input for the OPEM and CMAQ models. The analysis nudging technique (Jeon et al., 2015; Li et al., 2016) was applied to improve the performance of WRF modeling. The detailed configurations for WRF and CMAQ simulations are listed in Table 1 and 2, respectively.

3. Study method

A schematic flowchart of the modeling algorithm is depicted in Fig. 3. HGB area (Fig. 1) was chosen to be the simulation domain for this study. This area has already been the focus of several air quality modeling studies because of the unique mix of anthropogenic and biogenic sources (e.g., Pan et al., 2015; Diao et al., 2016; Souri et al., 2016).

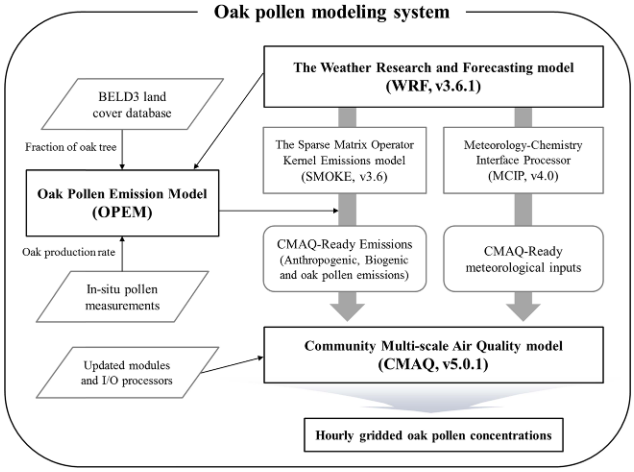

Fig. 3. Schematic flowchart describing the data and methodology within the OPEM-CPM modeling system.

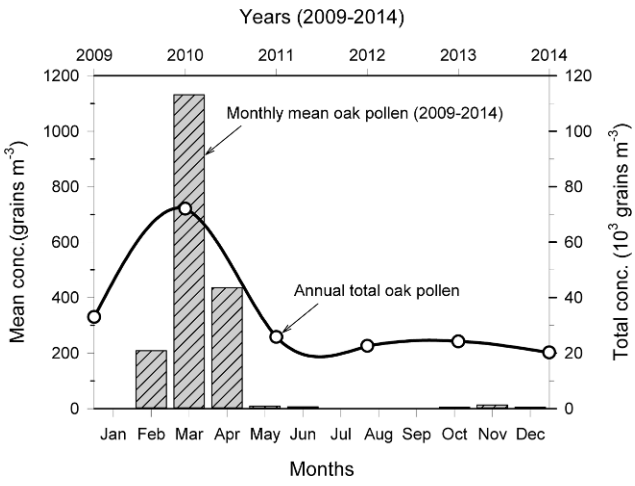

Fig. 4. Variation of monthly mean and annual total oak pollen concentrations during the period of 2009 to 2014.

The authors studied the historical pollen trends in Houston to decide the appropriate simulation period for this study. Figure 4 plots the monthly and annual variation of oak pollen concentrations during 2009-2014 at the TMC site in downtown Houston. The monthly mean oak pollen concentrations were relatively higher in the spring and late winter time and showed the highest value in March. The other periods except for spring and late winter showed negligible concentrations because the oak trees bloom at the beginning of spring (Pasken and Pietrowicz, 2005; Schueler and Schlünzen, 2006). The annual variation of mean oak pollen concentration during March in each year (Fig. 4) did not show clear trends, and the value in 2010 was the highest during the six-year period. Hence we selected three months from February to April in 2010, which showed markedly high concentrations of oak pollen to evaluate modeling performance for high oak pollen episodes. We set the onset day of oak pollen to February 21 based on the observational data at TMC site, and the simulations were conducted for the period from the onset day (February 21) to the end of April in 2010. We used several statistical parameters such as Index of Agreement (IOA), Mean Bias Error (MBE), and Normalized Root Mean Square Error (NRMSE) in this study for a quantitative evaluation of modeling performance.

4. Results

a. Simulated oak pollen emissions by OPEM

This section is intended to explain the spatial distribution of simulated oak pollen emissions. The gridded (1 km × 1 km) area fractions (%) of oak tree (i.e., aggregate oak species) obtained from the Biogenic Emissions Land use Database, version 3 (BELD3) dataset were converted to area values (1 m × 1 m) for use in the OPEM model. As shown in Fig. 5, the area with abundant vegetation (Fig. 1) showed higher oak fraction than other areas; e.g. the urbanized area showed a small fraction. Figure 6 shows distributions of the averaged daytime and nighttime oak pollen emission fluxes per each grid cell during the entire simulation period, calculated by OPEM. The distribution of emission fluxes strongly coincided with oak fraction because the total emission flux in each grid cell is proportional to the fraction of oak trees. Interestingly, the calculated oak pollen emissions in the Houston area were high despite of minimal oak fractions. The high surface temperature and wind speed, causing the high oak pollen emissions with increased K_e, did not appear in the area (Not shown). Hence the high emissions were very likely due to the noticeably high friction velocity values in the Houston area (Fig. 7): the calculated emission flux is proportional to friction velocity as described in Section 2.a. The simulated emission

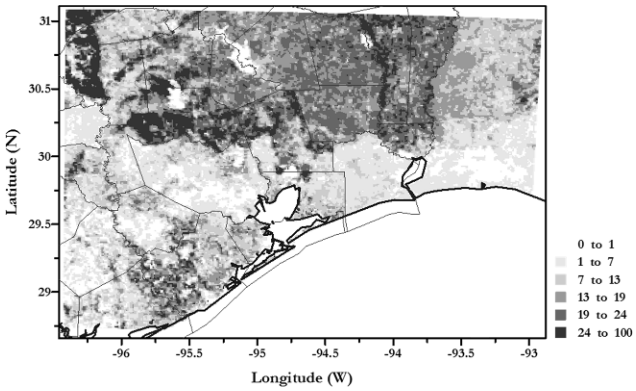

Fig. 5. Fraction (%) map of the oak tree within the HGB domain. The data for areal coverage of oak tree were obtained from the BELD3 database.

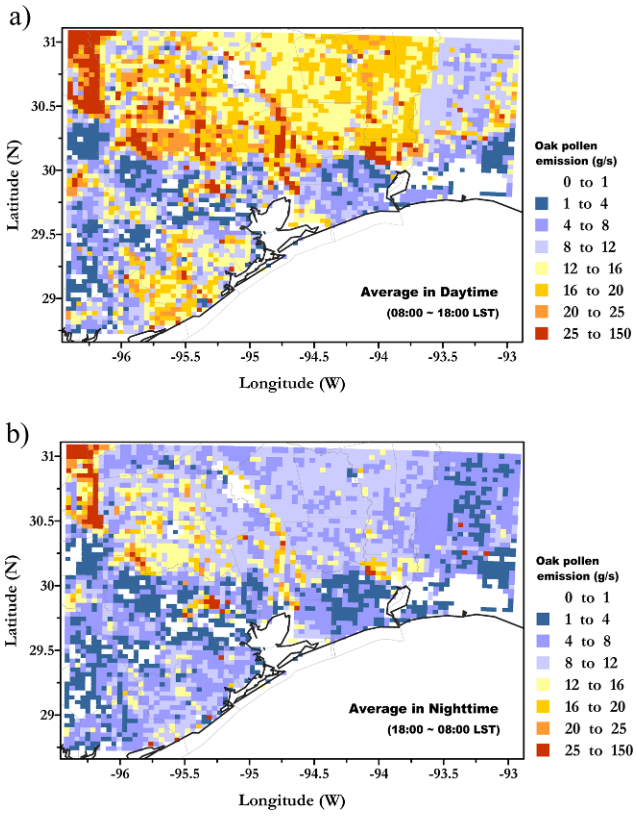

Fig. 6. Horizontal distribution of OPEM simulated oak pollen emissions during the a) day and b) night. The values are averages for the whole period of the episode (February 21-April 30).

rates in daytime were relatively higher than nighttime due to the higher temperature, wind speed and friction velocity. We should note that the significantly important role of friction velocity in the estimation of oak pollen emissions could be controversial because the estimated emissions might be inaccurate. Therefore, additional comparison studies with a different parameterization (e.g., Zink et al., 2013), based on

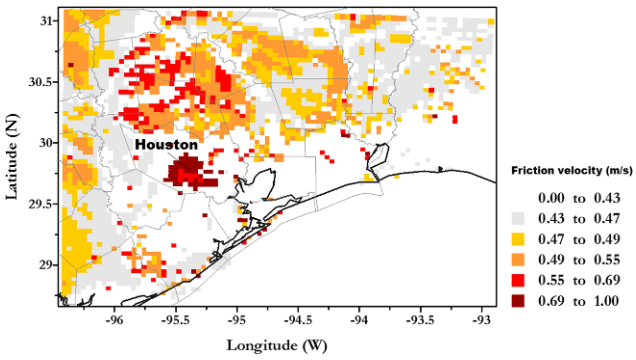

Fig. 7. Horizontal distribution of WRF simulated friction velocities. The values are averages for the whole period of the episode (February 21-April 30).

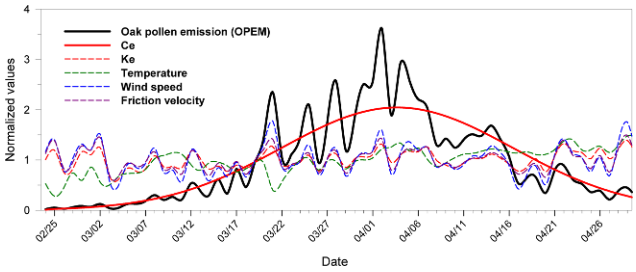

Fig. 8. Variation of the simulated oak pollen emission by the OPEM, the calculated $\boldsymbol{C_e}$, $\boldsymbol{K_e}$, temperature, wind speed, and friction velocity values during the whole episode period.

Table 3. The correlation coefficient (COR) between oak pollen emission and respective factors. The different COR values corresponding to four specific C_e range were separately listed.

	C_e	K_e	T	WS	u_*
[COR] Ce > 0.000	0.89	0.39	0.28	0.39	0.35
Ce > 0.010	-	0.49	0.08	0.65	0.62
Ce > 0.015	-	0.65	0.11	0.69	0.68
Ce > 0.020	-	0.82	0.20	0.79	0.82

turbulent kinetic energy (TKE) for the estimation of pollen lifting need to be conducted to evaluate the results from OPEM simulation.

Figure 8 plots the time series of hourly averaged oak pollen emission rate and the respective contributing factors to its variation during the simulation episode. All of the values were normalized to equalize the different units and data range for each factor. The oak pollen emission increased after the onset day and showed the first peak on March 20. The emissions showed the highest value on April 1. After which they started to decrease, approaching zero by the end of April. The temporal variation of the emissions coincided with that of C_e. As seen in Table 3, the correlation coefficient (COR) between the OPEM simulated emission rates and C_e values was quite

high (0.89), indicating that C_e plays a key role in the variation of oak pollen emissions. The COR of K_e (0.39), temperature (0.28), wind speed (0.39), and u_* (0.35) were relatively lower than that of C_e, reflecting that the impact of meteorology on the variation of oak pollen emission is not significant compared to C_e.

Interestingly, the COR of each meteorological factor varied within a specific range of C_e. For the time period of February 21 to April 30, when $C_e > 0.000$, the correlation between oak pollen emissions and K_e, T, wind speed (WS) and u_* was lower than 0.4, but it became higher as the C_e value increased. For the time period of $C_e > 0.020$, the correlation coefficients of K_e, T, WS and u_*, with oak pollen emissions were 0.82, 0.20, 0.79 and 0.82, respectively.

These results imply that the meteorological factors K_e, WS and u_*, which are related to the wind speed played an important role in the variation of oak pollen emission, especially during the days with high C_e values (i.e., high oak pollen emission days). The important role of wind speed on the variation of pollen concentration because of its close relation to u_* was reported by several previous studies using similar methodologies (Helbig et al., 2004; Vogel et al., 2008; Efstathiou et al., 2011); our results are consistent with theirs. The influence of air temperature on the variation of oak pollen emission was relatively minimal compared to that of wind speed.

As seen in Fig. 8, the daily variations of K_e, WS and u_* for the high emission days (March 18 to April 7) show good correlation with the pollen emission rate. The variation of air temperature showed positive correlation with that of oak pollen emissions, but it was relatively lower than those of other meteorological factors and it also did not showed consistent dependency of correlation according to the change in the C_e value.

To summarize, the emission rates of oak pollen simulated by OPEM were primarily driven by C_e and their daily variations were influenced by meteorological factors such as K_e, WS and u_*. While C_e drove the magnitude of emissions, meteorology determined their variability. Especially, the contribution of the meteorology to the variation of emissions increased with increasing emission rate.

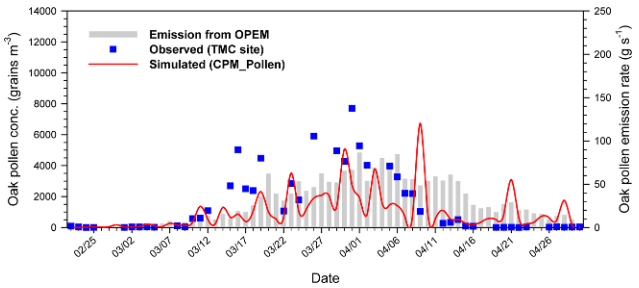

Fig. 9. Time series of the measured and the CPM simulated oak pollen concentrations (total values in each day) and the OPEM simulated oak pollen emission rate (average values in each day).

b. Simulated oak pollen concentrations by CPM

Figure 9 shows a comparison of time series between CPM-simulated oak pollen concentrations and in-situ measurements at the TMC site. The CPM accurately simulated the notable increase in oak pollen concentrations beginning on March 10. The modeled oak pollen concentrations were largely underestimated compared to the in-situ data, and failed to capture the peaks around March 16, 26, and 31.

Table 4 lists the calculated IOA, MBE, and NRMSE for the CPM simulated oak pollen concentrations during the period of simulation. The high IOA (0.75) reveals that the simulated oak pollen concentration by CPM showed similar temporal variation to that of the observations. We showed the MBE and NRMSE values as –479.81 grains m^{-3} and 24.82%, respectively. It means that the CPM underestimated oak pollen concentration and the simulated values have a mean error of 24.82% compared to observations. We need to be careful to conclude the reliable modeling performance of the CPM modeling because the model evaluation was performed using the measurement data obtained from a single site (TMC). It should be noted that only one pollen measurement site was available in the southeastern Texas area for this study. Thus, more evaluation work using adequate measurement data is needed to be performed in following studies to prove the

Table 4. Statistical summaries of the comparisons of the CPM simulation results with oak pollen observations across the entire period of the episode.

Statistical parameters		Mathematical expression[a]
Index of agreement	0.75	$\mathrm{IOA} = 1 - \frac{\Sigma_{i=1}^{N}(P_i - O_i)^2}{\Sigma_{i=1}^{N}(\lvert P_i - \overline{P}\rvert + \lvert O_i - \overline{O}\rvert)^2}$
Mean bias error (grains m^{-3})	–479.81	$\mathrm{MBE} = \frac{\Sigma_{i=1}^{N}(P_i - O_i)}{N}$
Normalized root mean square error (%)	24.82	$\mathrm{NRMSE} = \frac{100}{O_{i,max} - O_{i,min}}\sqrt{\frac{\Sigma_{i=1}^{N}(P_i - O_i)^2}{N}}$

[a] N is number of data points and P_i and O_i denote predicted and observed oak pollen concentrations, respectively.

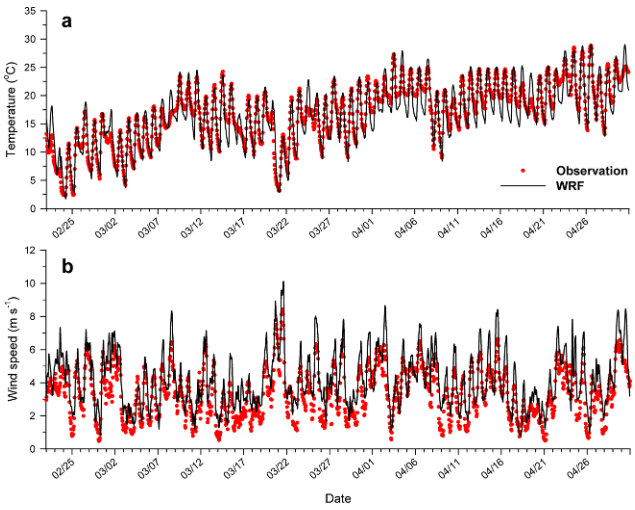

Fig. 10. Comparison between the observed and WRF simulated (a) mean temperature and (b) mean wind speed. The values are averages for all available CAMS sites (59 sites for temperature and 61 sites for wind speed) in the HGB domain.

reliable performance of CPM clearly.

5. Discussion

The inaccuracy of the oak pollen emissions generated by the OPEM probably caused the underestimation by the CPM. As seen in Fig. 9, the simulated oak pollen emissions did not capture the rapid increase concentrations on March 11. This discrepancy was likely due to the uncertainty of the C_e function. The magnitude of oak pollen emissions is strongly influenced by C_e, which did not perfectly represent the variation of oak pollen concentration after onset day at the TMC site as plotted in Fig. 1. Since the C_e function was calculated on the basis of a normal distribution, which is symmetric with a single peak, it did not take into account the multiple concentration peaks during the episode. For example, the observed oak pollen concentrations have two major peaks (March 15 and 30) but the OPEM simulated emissions did not accurately reproduce the two peaks because the C_e function used a normal distribution with a single peak.

As depicted in Fig. 10, the simulated air temperature and wind speed agreed well with the Texas Commission on Environmental Quality (TCEQ)'s Continuous Ambient Monitoring Stations (CAMS) data in the HGB domain, but they had only a marginal effect on the variation of oak pollen during the low C_e episodes. The current equation for the calculation of oak pollen emission used in OPEM may need to be updated in order to mitigate the strong dependence of the simulated emissions on the C_e value. An additional weighting factor that can magnify the effect of meteorology on the simulated oak pollen emission could possibly be adopted.

Another reason for the underestimation could be the drawback of the parameterization used in OPEM simulation. The parameterization utilized friction velocity as a governing parameter and did not specifically take into account the height of trees and other vegetation. The faulty consideration of the threshold mechanical stress related to pollen release was a likely cause of the underestimated pollen concentrations. Tall plants need relatively lower threshold mechanical stress to release pollen than shorter plants, and leaves on tall trees keep released pollen within the canopy (Zink et al., 2013). Consequently, considering the tree species-specific height in the parameterization could potentially mitigate the underestimated pollen concentration simulated by the CPM model. Uncertainty in the lateral pollen boundary condition could also be a reason for the underestimation. The CPM simulation with a single 4 km domain did not consider possible transport of oak pollen from outside the HGB domain, which could be a non-negligible factor in pollen simulations as suggested by Zink et al. (2012). Moreover, the uncertainties in the LAI, mean canopy height values, oak fractions from WRF simulation, literature (Burian et al., 2004), and BELD3 data might be the possible reasons for the inaccurate pollen estimates.

Interestingly, the CPM model over-predicted the oak pollen concentrations during the later period in April (8-30). In particular, the simulated concentrations on April 9, 21 and 28 were significantly overestimated. The function for defining C_e in Eq. (2) was based on climatology. Since the C_e curve was calculated by averaging all the flowering stages of oak pollen during the recent six years (2009-2014), it did not exactly take into account the shorter flowering season in 2010. The annual mean C_e curve cannot perfectly represent all the flowering seasons in each year and this is one of the key limitations of climatologic approach as addressed by Sofiev et al. (2006). Hence more pollen modeling and evaluation studies for this region using different methodologies (e.g., Zink et al., 2013) should be followed to provide comparison results that help to figure out a primary reason for the overestimated and/or underestimated oak pollen concentrations.

Favorable simulated meteorological conditions (i.e., high air temperature and wind speed) and uncertainty in simulated oak pollen emissions could be possible reasons behind the overestimation on April 21 and 28. Both oak pollen emissions and meteorological factors such as K_e, T, WS and u_* (Fig. 8) showed high values on April 21 and 28. However, the large difference between simulated and observed oak pollen concentrations on April 9 cannot be explained by the reason mentioned above. The simulated oak pollen emissions and meteorological factors did not show the peak on that day. Thus the poorly simulated oak pollen concentration on April 9 was likely due to the uncertainty in the wind fields from the WRF simulation, which play an important role in the transport of pollen concentration as indicated by Rojo et al. (2015). As shown in Fig. 11, the temporal variation of simulated wind vectors on April 9 did not reproduce the in-situ measurements correctly, especially from 03:00 to 09:00 a.m. During that time, the WRF-simulated wind was northeasterly, differing from the observed which ranged from easterly to southeasterly. The simulated northeasterly wind caused the transport of oak

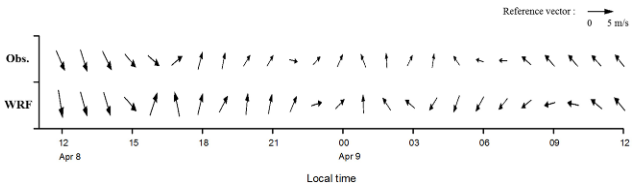

Fig. 11. Comparison between the observed and WRF simulated mean wind vectors on April 9 in 2010. The values are averages for all available CAMS sites (61 sites) in the HGB domain.

pollen from the forest regions (northeast part of the HGB domain) to Houston area and it resulted in the significantly overestimated oak pollen concentration on April 9.

In summary, the oak pollen emission rates calculated by OPEM primarily influenced the simulated oak pollen concentrations, but other factors such as meteorology and lateral boundary conditions also played a critical role for the simulated oak pollen concentrations, especially for transport.

6. Summary

An oak pollen simulation using the Oak Pollen Emission Model (OPEM) and CMAQ-Pollen Model (CPM) was conducted over the Houston-Galveston-Brazoria (HGB) area for the period of February 21 to April 30 in 2010, which showed significantly high concentrations of oak pollen. A dimensionless plant-specific factor describing the flowering period (C_e) primarily determined the simulated oak pollen emission rates by OPEM; the diurnal variation of emissions was influenced by meteorological factors such as the dimensionless meteorological adjustment factor (K_e), wind speed, and friction velocity. While C_e was critical for the magnitude of the amount of oak pollen emissions, meteorology determined their variability. In particular, the contribution of the meteorology to the variation of oak pollen emissions became increased with oak pollen emission rate. However, the CPM did not accurately reproduce the multi peaks of oak pollen concentrations. The model error was mainly due to the drawback of climatology-based C_e which cannot consider the characteristics of pollen flowering stages in each year.

We conclude that the OPEM framework needs to take into account the effect of meteorology on the variations of oak pollen simulation on a larger scale, and further evaluation studies using more detailed and updated input data should be performed. Additionally, the modeling results from the OPEM-CPM modeling system should be compared with those from the newly developed modeling approaches to better understand the limitations of this study and layout a future research direction following this study.

Acknowledgements. This study was funded by the Data Analytics in Student Hands Program at the Honors College and the Department of Earth and Atmospheric Sciences (HEAF FS 13 NSM CHOI and EAS Research Grant) of the University of Houston. This study was also supported by funding from the Environmental Health Center of the Ministry of Environment, Republic of Korea. The authors would like to thanks Amir Souri at UH, Alex Guenther at UCI, and Serena Chung at WSU for their useful guidance on the pollen studies.

Edited by: Tianjun Zhou

References

Burian S. J., S. W. Stetson, W. S. Han, J. Ching, and D. Byun, 2004: High-resolution dataset of urban canopy parameters for Houston, Texas. Preprint *Proc. Fifth Symposium on the Urban Environment*, Vancouver, American Meteorological Society, CD 9.3.

Byun, D., and K. L. Schere, 2006: Review of the governing equations, computational algorithms, and other components of the Models-3 Community Multiscale Air Quality (CMAQ) modeling system. *Appl. Mech. Rev.*, **59**, 51-77.

Després, V. R., and Coauthors, 2012: Primary biological aerosol particles in the atmosphere: A review. *Tellus*, **64**, 15598, doi:10.3402/tellusb.v64i0.15598.

Diao, L., Y. Choi, B. Czader, X. Li, S. Pan, A. Roy, A. H. Souri, M. Estes, and W. Jeon, 2016: Discrepancies between modeled and observed nocturnal isoprene in an urban environment and the possible causes: A case study in Houston. *Atmos. Res.*, **181**, 257-264, doi:10.1016/j.atmosres.2016.07.009.

Dupont, S., Y. Brunet, and N. Jarosz, 2006: Eulerian modelling of pollen dispersal over heterogeneous vegetation canopies. *Agr. Forest Meteor.*, **141**, 82-104.

Efstathiou, C., S. Isukapalli, and P. Georgopoulos, 2011: A mechanistic modeling system for estimating large-scale emissions and transport of pollen and co-allergens. *Atmos. Envrion.*, **45**, 2260-2276, doi:10.1016/j.atmosenv.2010.12.008.

Helbig, N., B. Vogel, H. Vogel, and F. Fiedler, 2004: Numerical modelling of pollen dispersion on the reginal scale. *Aerobiol.*, **20**, 3-19.

Houyoux, M., J. Vukovich, and J. Brandmeyer, 2000: Sparse Matrix Kernel Emissions Modeling System: SMOKE User Manual, MCNC-North Carolina Supercomputing Center. [available online at http://www.cmascenter.org.]

Jarosz, N., B. Loubet, and L. Huber, 2004: Modelling airborne concentration and deposition rate of maize pollen. *Atmos. Environ.*, **38**, 5555-5566.

Jato, V., F. J. Rodríguez-Rajo, and M. J. Aira, 2007: Use of Quercus ilex subsp. ballota phenological and pollen-production data for interpreting Quercus pollen curves. *Aerobiol.*, **23**, 91-105.

Jeon, W., Y. Choi, H. W. Lee, S.-H. Lee, J.-W. Yoo, J. Park, and H.-J. Lee, 2015: A quantitative analysis of grid nudging effect on each process of $PM_{2.5}$ production in the Korean Peninsula. *Atmos. Environ.*, **122**, 763-774, doi:10.1016/j.atmosenv.2015.10.050.

Knox, R. B., C. Suphioglu, P. Taylor, R. Desai, H. C. Watson, J. L. Peng, and L. A. Bursill, 1997: Major grass pollen allergen Lol p 1 binds to diesel exhaust particles: implications for asthama and air pollution. *Clin. Exp. Allergy*, **27**, 246-251.

Lamb, C. E., P. H. Ratner, C. E. Johnson, A. J. Ambegaonkar, A. V. Joshi, D. Day, N. Sampson, and B. Eng, 2006: Economic impact of workplace productivity losses due to allergic rhinitis compared with select medical conditions in the United States from an employer perspective. *Curr. Med. Res. Opin.*, **22**, 1203-1210.

Li, X., Y. Choi, B. Czader, A. Roy, H. Kim, B. Lefer, and S. Pan, 2016: The impact of observation nudging on simulated meteorology and ozone concentrations during DISCOVER-AQ 2013 Texas campaign. *Atmos. Chem. Phys.*, **16**, 3127-3144, doi:10.5194/acp-16-2016.

Motta, A. C., M. Marliere, G. Peltre, P. A. Sterenberg, and G. Lacroix, 2006: Traffic-related air pollutatns induce the release of allergen-containing cytoplasmic granules from grass pollen. *Int. Arch. Allergy Imm.*, **139**, 294-298.

Nathan, R., E. Meltzer, J. Seiner, and W. Storms, 1997: Prevalence of allergenic rhinitis in the United States. *J. Allergy Clin. Immun.*, **99**, 808-814.

Oh, I., Y. Kim, K.-R. Choi, M. Suzuki, and J. Lee, 2012: Pollen simulations in a coastal urban area of Ulsan, Korea: Preliminary results using WRF-CMAQ model. *Proc. of the 13th International Palynological Congress and 9th International Organization of Palaeobotany Conference,* Tokyo, Japan, Paper No.SS28-O05.

Pan, S., Y. Choi, A. Roy, X. Li, W. Jeon, and A. H. Souri, 2015: Modeling the uncertainty of several VOC and its impact on simulated VOC and ozone in Houston, Texas. *Atmos. Environ.*, **120**, 404-416, doi:10.1016/j.atmosenv.2015.09.029.

_____, _____, W. Jeon, A. Roy, D. A. Westenbarger, and H. C. Kim, 2017: Impact of high-resolution sea surface temperature, emission spikes and wind on simulated surface ozone in Houston, Texas during a high ozone episode. *Atmos. Environ.*, **152**, 362-376, doi:10.1016/j.atmosenv.2016.12.030.

Pasken, R., and J. A. Pietrowicz, 2005: Using dispersion and mesoscale meteorological models to forecast pollen concentrations. *Atmos. Environ.*, **39**, 7689-7701.

Pfender, W., R. Graw, W. Bradley, M. Carney, and L. Maxwell, 2007: Emission rates, survival, and modeled dispersal of viable pollen of creeping bent grass. *Crop Sci.*, **47**, 2529-2539.

Rojo, J., and R. Perez-Badia, 2015: Spatiotemporal analysis of olive flowering using geostatistical techniques. *Sci. Total Environ.*, **505**, 860-869, doi:10.1016/j.scitotenv.2014.10.022.

Rojo, J., A. Rapp, B. Lara, F. Fernández-González, and R. Pérez-Badia, 2015: Effect of land uses and wind direction on the contribution of local sources th airborne pollen. *Sci. Total Environ.*, **538**, 672-682, doi:10.1016/j.scitotenv.2015.08.074.

Saito, H., M. Okubo, and J. Kunitomo, 2006: Pollen production of a Qeuercus pshillyraeoides stand in Shodo-shima Island. Kagawa. *Japan. J. Palynology*, **52**, 47-52.

Schoenwetter, W., L. Dupclay, S. Appajosyula, M. F. Botteman, and C. L. Pashos, 2004: Economic impact and quality-of-life burden of allergic rhinitis. *Curr. Med. Res. Opin.*, **20**, 305-317.

Schueler, S., and K. H. Schlünzen, 2006: Modeling of oak pollen dispersal on the landscape level with a mesoscale atmospheric model. *Environ. Model Assess.*, **11**, 179-194.

Sofiev, M., P. Siljamo, H. Ranta, and A. Rantio-Lehtimäki, 2006: Towards numerical forecasting of long-range air transport of birch pollen: theoretical considerations and a feasibility study. *Int. J. Biometeorol.*, **50**, 397-402.

Souri, A. H., Y. Choi, W. Jeon, X. Li, S. Pan, L. Diao, and D. A. Westenbarger, 2016: Constraining NOx emissions using satellite NO_2 measurements during 2013 DISCOVER-AQ Texas campaign. *Atmos. Environ.*, **131**, 371-381, doi:10.1016/j.atmosenv.2016.02.020.

Stanley, R. G., and H. F. Linskens, 2012: *Pollen: Biology Biochemistry Management*. Springer Science & Business Media, 310 pp.

Taylor, P. E., K. W. Jacobson, J. M. House, and M. M. Glovsky, 2007: Links between pollen, atopy and the asthma epidemic. *Int. Arch. Allergy Imm.*, **144**, 162-170, doi:10.1159/000103230.

Vogel, B., F. Fiedler, and H. Vogel, 1995: Influence of topography and biogenic volatile organic compounds emission in the state of Baden-Württemberg on ozone concentrations during episodes of high air temperatures. *J. Geophys. Res.*, **100**, 22907-22928.

_____, H. Vogel, D. Bäumer, M. Bangert, K. Lundgren, R. Rinke, and T. Stanelle, 2009: The comprehensive model system COSMO-ART - Radiative impact of aerosol on the state of the atmosphere on the regional scale. *Atmos. Chem. Phys.*, **9**, 8661-8680, doi:10.5194/acp-9-8661-2009.

Vogel, H., A. Pauling, and B. Vogel, 2008: Numerical simulation of birch pollen dispersion with an operational weather forecast system. *Int. J. Biometeorol.*, **52**, 805-814.

Veriankaitė, L., P. Siljamo, M. Sofiev, I. Šaulienė, and J. Kukkonen, 2010: Modeling analysis of source regions of long-range transported birch pollen that influences allergenic seasons in Lithuania. *Aerobiol.*, **26**, 47-62, doi:10.1007/s10453-009-9142-6.

Zink, K., H. Vogel, B. Vogel, D. Magyar, and C. Kottmeier, 2012: Modeling the dispersion of Ambrosia artemisiifolia L. pollen with the model system COSMO-ART. *Int. J. Biometeorol.*, **56**, 669-680, doi:10.1007/s00484-011-0468-8.

_____, A. Pauling, M. W. Rotach, H. Vogel, P. Kaufmann, and B. Clot, 2013: EMPOL 1.0: A new parameterization of pollen emission in numerical weather prediction models. *Geosci. Model Dev.*, **6**, 1961-1975, doi:10.5194/gmd-6-1961-2013.